

## PHASE COMPOSITION AND CRYSTALLINITY OF HYDROXYAPATITE WITH VARIOUS HEAT TREATMENT TEMPERATURES

DECKY J INDRANI<sup>1\*</sup>, BAMBANG SOEGIJONO<sup>2</sup>, WISNU A ADI<sup>3</sup>, NEIL TROUT<sup>4</sup>

<sup>1</sup>Department of Dental Materials Science, Faculty of Dentistry, Universitas Indonesia, Jakarta, Indonesia. <sup>2</sup>Department of Physics, Faculty of Mathematics and Natural Sciences, Universitas Indonesia, Jakarta, Indonesia. <sup>3</sup>Department of , Center for Science and Technology of Advanced Materials, National Nuclear Energy Agency, Banten, Indonesia. <sup>4</sup>Department of University of South Australia, Adelaide, Australia. Email: deckyji@gmail.com

Received: 16 September 2017, Revised and Accepted: 3 October 2017

### ABSTRACT

**Objective:** This study investigated effects of heat treatment on the crystallinity and phase composition of hydroxyapatites (HAs) of different heat treatment.

**Methods:** HA powder was synthesized by the chemical precipitation method based on the reaction between the phosphorous acid and calcium hydroxide. Synthesized HA was divided into three groups for which each group was then given heat treatment at 100°C, 900°C, or 1300°C. Phase identification, analyses and the crystallinity of the synthesized HAs were determined using the X-ray diffraction coupled with the Rietveld refinement.

**Results:** The synthesized HAs with each heat treatment were identified as HA phase containing hexagonal structure. Those treated at 100°C or 900°C revealed with crystallinity of 48% and 68%, respectively, with no additional phase; whereas, those treated at 1300°C produced a crystallinity of 72% and contained dicalcium and tricalcium phosphates.

**Conclusion:** The synthesized HAs treated at 100°C, 900°C, or 1300°C were HA phase with hexagonal structure. The variable crystallinity of the synthesized HAs yielded from different heat treatment temperature correspondingly determines different phase composition.

**Keywords:** Amorphous, Crystallinity, Heat treatment, Hydroxyapatite, Secondary phase.

© 2017 The Authors. Published by Innovare Academic Sciences Pvt Ltd. This is an open access article under the CC BY license (<http://creativecommons.org/licenses/by/4.0/>) DOI: <http://dx.doi.org/10.22159/ijap.2017.v9s2.21>

### INTRODUCTION

One may suffer from bone destruction due to tooth extraction or physiological alveolar bone resorption in elderly patients for which these conditions need to be treated. For bone regeneration treatment, tissue engineering is considered as a promising alternative approach [1-3]. In this approach, tissue engineering has particularly been using an artificial device (scaffold), functions as a template to support and guide the growth of cells through the porous structures, implanted in bone defects in a patient's body [3,4]. Scaffold materials, therefore, have to mimic a normal calcified tissue of human bone, the biological apatite. The most similar calcium phosphate-based bioceramics to biological apatite has been hydroxyapatite (HA), having a molecular formula of  $\text{Ca}_{10}(\text{PO}_4)_6(\text{OH})_2$ , with a molar ratio of Ca/P 1.67 and showing the most similar crystallography [5-7].

HAs with high heat treatment have been studied. High heat treatment led to grain growth and densification which increased their crystallinity, to obtain high mechanical strength, suitable for orthopedics applications. For example, synthesized HA with a heat treatment up to 1200°C demonstrated an increase in hardness and fracture strength [8]. Further heat treatment of HA up to 1250°C has resulted with even superior hardness and fracture toughness [9]. Despite being advantageous, limitations remain in the difficulty for a crystalline HA. The successful growth of cells cultured in a scaffold requires the scaffold being degradable, to be resorbable [3,4].

Efforts to raise degradability of a scaffold have been studied using an amorphous HA. Calcium phosphate-based phases are having a molar ratio of Ca/P <1.7, such as tricalcium phosphate, have shown to be more degradable. Studies showed that biphasic structure of HA and tricalcium phosphate (HA/TCP) have drawn considerable attention because they

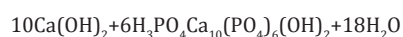
are able to show better degradation [3,10,11]. In fact, most studies of biphasic HA/TCP scaffold employed commercially available HAs. Commercially available HAs possessed the heat treatment estimated to be between 900°C and 1300°C [12].

Crystallinity of HA is considered as an important parameter as the degradability of a scaffold is strongly dependent on them. Crystalline HA is bioinert and less degradable when it is used for scaffolds. On the other hand, very low heat treatment of HA may result with an amorphous effect; in addition, their degradation in the form of micro-particle released is feared to cause cellular damages occurring around an implanted scaffold. To gain insights into crystalline HA for scaffold applications for tissue engineering, it is important to analyze the crystallinity and phase composition of a synthesized HA. Therefore, this study aims to explore the crystallinity and phase of the composition of HA with different heat treatments.

### METHODS

#### Synthesis of HA powders

The reagents used were calcium hydroxide [ $\text{Ca}(\text{OH})_2$ ] and orthophosphoric acid [ $\text{H}_3\text{PO}_4$ ]. All analytical grade reagents used in this work were purchased from Sigma-Aldrich (St. Louis, Missouri, USA). Synthesis of HA was conducted using the wet chemical precipitation method, following previous studies [9,13-15]. In brief,  $\text{H}_3\text{PO}_4$  and  $\text{Ca}(\text{OH})_2$  were as shown in the chemical reaction below:



The mixing was conducted by addition of  $\text{H}_3\text{PO}_4$  powder into  $\text{Ca}(\text{OH})_2$  suspension in water in a dropwise manner and a controlled rate for 1 h. Vigorous mixing was carried out by continued stirring on a magnetic

stirrer (Heidolph MR 3001, Germany) at  $\pm 900$  rpm and maintained for 24 h. At the end of the stirring process, pH of the mixture was 11–12 and was then adjusted to pH 7. The mixture was aged overnight; wet cakes produced from the precipitate were subjected to filtering adapted in a Büchner funnel until dry and were repeatedly washed with deionized water. After further drying in a furnace, dried cakes at the bottom were ground into fine powder and were then divided into three groups and each group was given a heat treatment at 100°C, 900°C, or 1300°C, with a stepwise of 0.5°C/min and maintained for 3 h before furnace-cooled down to room temperature. A commercially available HA (Sigma-Aldrich, St. Louis, Missouri, USA) was used as a comparison.

#### X-ray diffraction (XRD) and crystallinity determination

Synthesized HA powder was prepared in molds of 25 mm in inner diameter and 2 mm in thickness to produce samples. The samples were mounted in and scanned with an XRD (PW-1170, Phillips, Netherland), with Cu-K $\alpha$  and  $\lambda = 1.5406$  Å. Data from the samples were collected in the  $2\theta$  range from 10 to 80° by step counting at 0.02 deg. intervals for 0.6 seconds per data point. The XRD coupled with the Rietveld refinement, as implemented in the GSAS program, was utilized to obtain the lattice parameter. It was also used to measure the crystallinity of each group, which was measured from a crystalline to the total area, including the amorphous phase; the crystalline area is the sum of the integrated intensities scattered over a suitable angular interval by crystalline phase. It was also used to detect the existence of secondary phases by comparing the diffraction patterns of the synthesized HA with the International Centre for Diffraction Data (ICDD; Newtown Square, PA) File Card No. 09-0432 for Ca<sub>10</sub>(PO<sub>4</sub>)<sub>6</sub>(OH)<sub>2</sub> (HA), File Card No. 96-100-1557 for Ca<sub>2</sub>P<sub>2</sub>O<sub>7</sub> (dicalcium phosphate [DCP]), File Card No. 96-900-5866 for Ca<sub>3</sub>(PO<sub>4</sub>)<sub>2</sub> (tricalcium phosphate), and File Card No. 44-1481 for CaO (calcium oxide).

#### RESULTS

The synthesis of HA obtained from the chemical precipitation method used in this study was confirmed by XRD patterns, as was shown in Fig. 1.

As in Fig. 1, characteristic peaks of each pattern were attributed to the crystallographic planes at (002), (210), (211), (112), (300), (202), (310), (222), (213), (004), and (304). All the peaks can be matched with the ICDD no. 09-0432 for HA. The XRD pattern displayed evident similarities in their characteristic peaks; however, there were differences observed from peak broadening (Fig. 1). In correspondence with the view, the synthesized HA with heat treatment at 100°C were observed with broad peaks. It was estimated that at 100°C, the synthesized HA was contributed by less grain growth, less perfect crystal in the range of Angstroms showing microcrystalline particles of a large fraction of a poorly crystallized material. Further increasing to 900°C, narrow peaks were observed with enhanced resolution and they became sharper at 1300°C. Here, the synthesized HA were likely to result with large particles. Further identification of HA using the Rietveld refinement showed the lattice parameters and the crystallinity values, as were shown in Table 1.

As we can see in Table 1, the lattice parameter of each synthesized HA phase with different heat treatment. The parameters = 90° and 120° confirmed the hexagonal crystal structure with the space group of P63/m (ICDD File Card No. 09-0432).

The parameters displayed increasing values, presenting the HAs were given increased heat treated. However, they displayed small variation

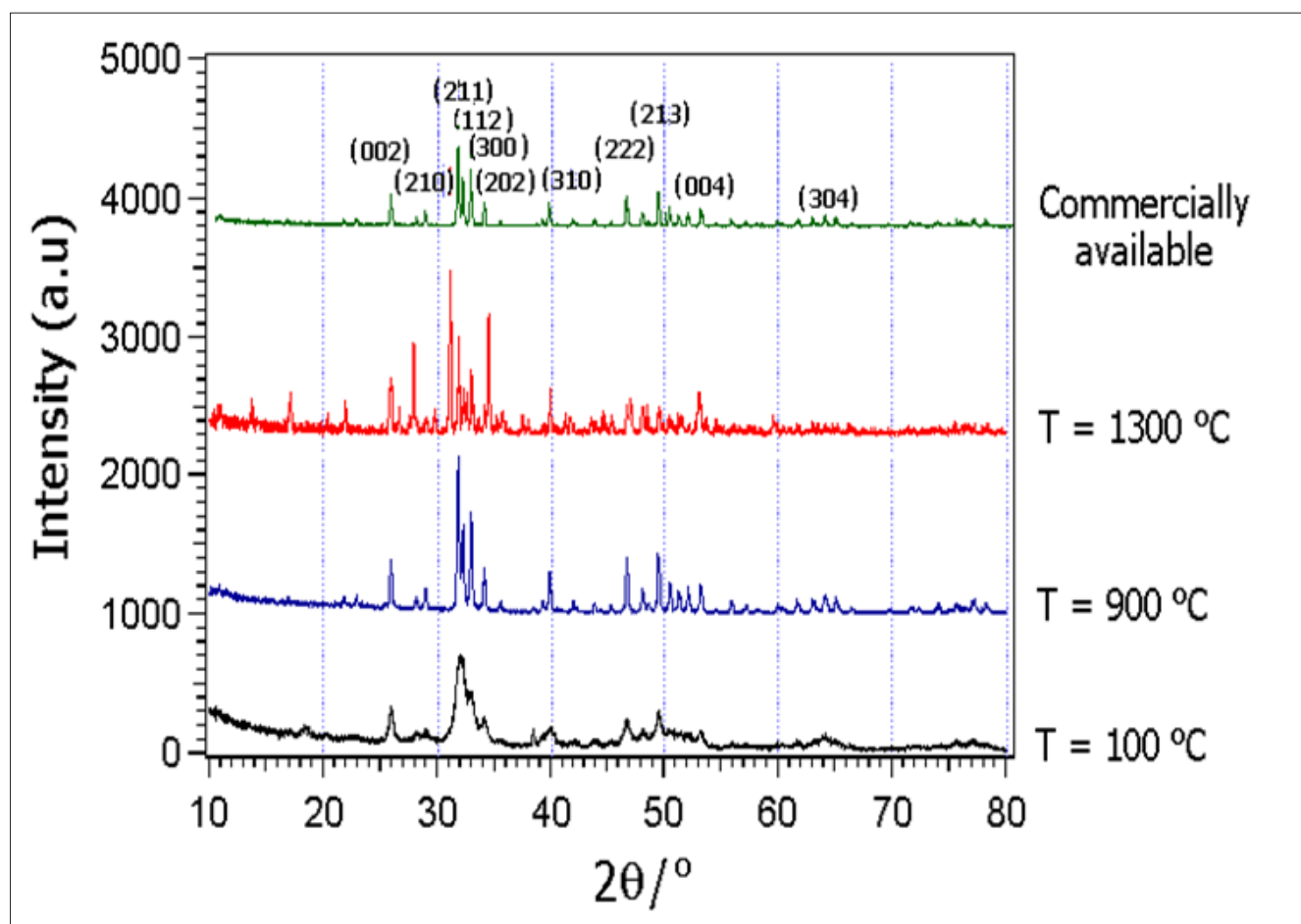


Fig. 1: X-ray diffraction patterns from the synthesized hydroxyapatite (HA) treated at 100°C, 900°C, or 1300°C and the commercially available HA

**Table 1: Lattice parameter and mass fraction of the synthesized HA-treated at 100°C, 900°C, or 1300°C and the commercially available HA**

Heat treatment of HA (°C)	Lattice parameter				Crystallinity (%)
	$\alpha = \beta \neq \gamma$ (°)		$a = b \neq c$ (Å)		
	$\gamma$ (°)	$a = b$ (Å)	$\gamma$ (°)	$c$ (Å)	
Synthesized					
100	90	120	9.404	6.902	48
900	90	120	9.406	6.977	65
1300	90	120	9.407	6.999	72
Commercially available	90	120		6.999	86

HA: Hydroxyapatite

compared to that obtained from the commercially available HA. These results were also accordance with those obtained from nano-sized HA particles [16,17]. With respect to the crystallinity, the synthesized HA samples with the heat treatment at 100°C have revealed with a value of 48%. Increasing the heat treatment to 900°C resulted with the crystallinity of 65%, which was raised by about 17% compared to that with 100°C. Further increasing the heat treatment to 1300°C has further elevated the crystallinity to nominally 72%, which was 7% higher than that with 900°C. When the commercially available HA with a crystallinity of 86% was considered, the crystallinity of the synthesized HA samples was known to be lower. The refinement allowed ensure better reliability and identification of the additional phases, as were seen in Fig. 2 and summarized in Table 2.

The XRD pattern in Fig. 2a showed that the synthesized HA with heat treatment at 100°C was accompanied with peaks attributed to planes at (111), (200), and (220). This was consistent with the ICDD Card File No. 44-1481 for CaO. As was seen in Table 2, the mass fraction of the CaO phase, however, was as low as 0.74%, which may not be a significant amount.

In Fig. 2b, the XRD pattern showed that the synthesized HA samples with heat treatment at 900°C (Table 2) came with no additional peak. Thus, they contained 100% HA phase. Regarding the commercially available HA (Fig. 2d), no other peak corresponding to any secondary phase was also seen, meaning that it contained 100% HA phase. The results showed that the synthesized HA-treated at 900°C and the commercially available were in accordance.

Heated at 1300°C (Fig. 2c), the synthesized HA samples demonstrated planes at (020), (023), (015), (009), (205), and (025) that can be indexed with the ICDD Card File No. 96-100-1557 for DCP. The planes at (022), (110), (202), and (008) agreed with ICDD Card File No. 96-900-5866 for tricalcium phosphate.

We found that the synthesized HA with heat treatment at 1300°C has produced main HA, DCP and tricalcium phosphate phases (Table 2). The mass fractions were noticed to be nominally 56.07%, 33.23%, and 10.70%, respectively. Although the apparent secondary phase was totally 43.93%, which was nearly similar to the main HA phase, the crystallinity noted to be 72% was still higher than that heated at 900°C.

## DISCUSSION

The XRD patterns occurred from each synthesized HA agreed well with those published in other literature. The XRD patterns were similar with those prepared using a similar method, either with similar reagents or different chemicals employed as were used in this study [9,13-15,18]. The analogies between the XRD patterns obtained from the synthesized HA and those from the commercially available HA showed that both resemble each other. These typical of HA was similar to that from a bovine bone as reported earlier [19,20].

The XRD pattern of the extracted HA from the bovine bone with heat treatment at 100°C, as previously described, was similar to that of the synthesized HA with the same heat treatment in this study.

**Table 2: Phases and mass fractions of the synthesized HA-treated at 100°C, 900°C, or 1300°C and the commercially available HA**

HA, heat treatment (°C)	Phase		Mass fraction (%)
	Main	Secondary	
Synthesized			
100	HA	Calcium oxide	99.26 0.74
900	HA		100.0
1300	HA	DCP TCP	56.07 33.23 10.70
Commercially available	HA		100.0

HA: Hydroxyapatite, DCP: Dicalcium phosphate, TCP: Tricalcium phosphate

The occurrence of CaO phase may be due to phosphorous containing precursors which are potentially volatile; hence, calcium-containing precursor molecules have difficulty to be incorporated into the complex. The synthesized HA samples with relatively low heat treatment at 100°C can be considered as poorly crystallized material (Table 1). As observed in Fig. 1, the change of the peaks from narrow at 900°C to broad at 100°C indicated that the change of the synthesized HA samples was from crystalline to amorphous.

The findings from this study were accordance to previous studies on applying high heat treatment to synthesized HAs that occurred with secondary phases, as presented by additional reflections on their XRD patterns. Ramesh *et al.* demonstrated that the formation of tricalcium phosphate and DCP phases when HA was heated at 1300°C was unavoidable [9]. A report mentioned that HA with lower heat treatment at 1200°C has also occurred with tricalcium phosphate phase [21]. With respect to the HA phase diagram, HA decomposed at around 1180°C [22]. It was also reported that the transformation of HA into tricalcium phosphate at a lower heat treatment of 1100°C [23].

Biodegradation of a scaffold occurs from the time of implantation *in vivo* to the completion of bone regeneration [24,25]. Controlling the biodegradation rate of any scaffold to match the bone tissues regeneration rate requires a balance between degradability and on the other hand a sufficient mechanical integrity. To obtain scaffolds with these requirements, one of the greatest challenges in tissue engineering should address a well-defined HA scaffold and observe the biodegradability and worth mentioning the mechanical integrity.

Tricalcium phosphate and DCP phases, having a molar ratio of Ca/P 1.5 and 1.43, respectively, have been the most used calcium phosphate to construct biphasic HA-based scaffolds [10]. In this study, the presence of tricalcium phosphate and DCP phases in the synthesized HA-treated at 1300°C was actually an advantage for the intention to raise biodegradability of the scaffold. However, HA-treated at 1300°C showed relatively high crystallinity. When in an implantation, the residual crystalline HA of the scaffold may escape from biodegradation. In this

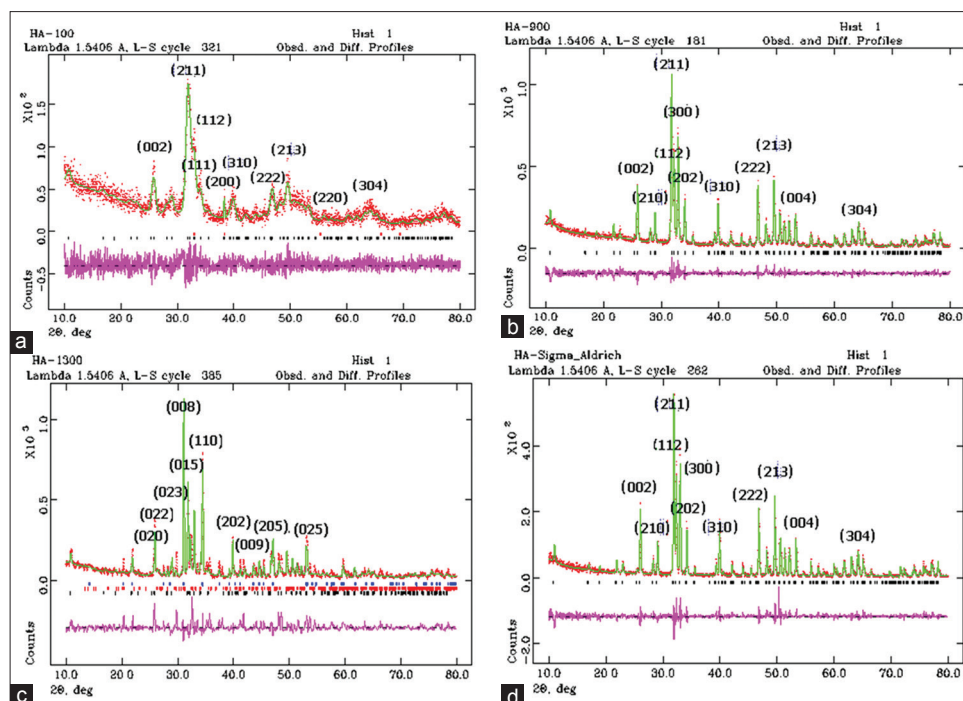


Fig. 2: Rietveld refinement of the synthesized hydroxyapatite (HA) treated at (a)100°C, (b)900°C, and (c)1300°C and (d) the commercially available HA showing main and secondary phases

case, HA-treated between 100°C and 900°C, such as obtained from this study, may be admired to obtain amorphous HA.

Furthermore, to obtain higher biodegradation of HA-based scaffolds, HA has been composited with biopolymer. In the past decade, polysaccharides, such as alginates and/or chitosan have been used in biomedical purposes [26,27]. Future studies, therefore, may develop scaffolds of HA combined with chitosan and/or alginate for tissue engineering.

## CONCLUSION

Synthesize HAs produced by the wet chemical precipitation and heat treated at 100°C, 900°C or 1300°C were identified as HA phase and shown to consist of the hexagonal crystal structure with the space group of P63/m. HAs treated at 1300°C was considered crystalline and contained dicalcium and tricalcium phosphate, whereas, those treated at 100°C or 900°C presented no significant amount of additional phase and was considered amorphous.

## ACKNOWLEDGMENT

The authors acknowledge the financial support from the Ministry of Research, Technology and Higher Education of Indonesia.

The publication of this manuscript is supported by Universitas Indonesia.

## REFERENCES

1. Bose S, Roy M, Bandyopadhyay A. Recent advances in bone tissue engineering scaffolds. *Trends Biotechnol* 2012;30:546-54.
2. Kumar P, Vinitha B, Fathima G. Bone grafts in dentistry. *J Pharm Bioallied Sci* 2013;5 Suppl 1:S125-7.
3. Al-Sanabani JS, Madfa AA, Al-Sanabani FA. Application of calcium phosphate materials in dentistry. *Trends Biotechnol* 2013;30:546-54.
4. Demirbag B, Huri PY, Kose GT, Buyuksungur A, Hasirci V. Advanced cell therapies with and without scaffolds. *Biotechnol J* 2011;6:1437-53.
5. Krishnamurthy GA. Review on hydroxyapatite-based scaffolds as a potential bone graft substitute for bone tissue engineering applications. *Short Commun Jummec* 2013;16:1-6.

6. Dorozhkin SV. Calcium orthophosphates as bioceramics: State of the art. *J Funct Biomater* 2010;1:22-107.
7. Zyman ZZ, Rokhmistov DV, Loza KI. Determination of the Ca/P ratio in calcium phosphates during the precipitation of hydroxyapatite using X-ray diffractometry. *Process Appl Ceram* 2013;7:93-5.
8. Al-Khazraji KK, Hanna WA, Ahmed PS. Effect of sintering temperature on some physical and mechanical properties of fabricated hydroxyapatite used for hard tissue healing. *Eng Technol J* 2010;28:1880-92.
9. Ramesh S, Tolouei SR, Tan CY, Aw KL, Yeo WH, Sopyan, *et al.* Sintering of hydroxyapatite ceramic produced by wet chemical method. *Adv Mater Res* 2011;264:1856-61.
10. Gallinetti S, Canal C, Ginebra I MP. Degradation and characterisation of new biphasic calcium phosphate cements. *Eur Cell Mater* 2012;23:6.
11. Komlev VS, Mastrogiacomo M, Pereira RC, Peyrin F, Rustichelli F, Cancedda R. Biodegradation of porous calcium phosphate scaffolds in an ectopic bone formation model studied by X-ray computed microtomograph. *Eur Cell Mater* 2010;19:136-46.
12. Nazarpak MH, Solati-Hashjin M, Moztafzadeh F. Preparation of hydroxyapatite ceramics for biomedical applications. *J Ceram Process Res* 2009;10:54-7.
13. Stipniccean L, Salma-Ancanea K, Borodajenka N, Sokolovab M, Jakovlevsb D, Berzina-Cimdinai L. Characterization of Mg-substituted hydroxyapatite synthesized by wet chemical method. *Ceram Int* 2014;40:3261-7.
14. Chandrasekar A, Sagadevan S, Dakshnamoorthy. Synthesis and characterization of nano-hydroxyapatite (n-HAP) using the wet chemical technique. *Int J Phys Sci* 2013;8:1639-45.
15. Monmaturapoj N. Nona-size hydroxyapatite powders preparation by wet-chemical precipitation route. *J Met Mater Miner* 2008;18:15-20.
16. Brundavanam RK, Poinern GE, Fawcett D. Modelling the crystal structure of a 30 nm sized particle based hydroxyapatite powder synthesised under the influence of ultrasound irradiation from x-ray powder diffraction data. *Am J Mater Sci* 2013;3:84-90.
17. Zannotto A, Saladino ML, Martino DC, Caponetti E. Influence of temperature on calcium hydroxyapatite nan powders. *Adv Nanoparticles* 2012;1:21-2.
18. Martínez-Castañón GA, Loyola-Rodríguez JP, Zavala-Alonso NV. Preparation and characterization of nanostructured powders of hydroxyapatite. *Superficies Vacío* 2012;25:101-5.
19. Manalu JL, Soegijono B, Indrani DJ. Characterization of hydroxyapatite derived from bovine bone Asian *J Appl Sci* 2015;3:758-65.
20. Kusriani E, Sontang M. Characterization of X-ray diffraction and electron spin resonance: Effects of sintering time and temperature on

- bovine hydroxyapatite. *Radiat Phys Chem* 2012;81:118-25.
21. Malina D, Biernat K, Sobczak-Kupiec A. Studies on sintering process of synthetic hydroxyapatite. *Acta Biochim Pol* 2013;60:851-5.
  22. White AA, Kinloch IA, Windle AH, Best SM. Optimization of the sintering atmosphere for high-density hydroxyapatite-carbon nanotube composites. *J R Soc Interface* 2010;7 Suppl 5:S529-39.
  23. Ou SF, Chiou SY, Ou KL. Phase transformation on hydroxyapatite decomposition. *Ceram Int* 2013;39:3809-16.
  24. Scalera F, Gervaso F, Sanosh KP, Sannino A, Licciulli A. Influence of the calcinations temperature on morphological and mechanical properties of highly porous hydroxyapatite scaffolds. *Ceram Int* 2013;39:4839-46.
  25. Duan H, Yang H, Xiong Y, Zhang B, Ren C, Min L. Effects of mechanical loading on the degradability and mechanical properties of the nanocalcium-deficient hydroxyapatite-multi (amino-acid) copolymer composite membrane tube for guided bone regeneration. *Int J Nanomed* 2013;8:2801-7.
  26. Shaji J, Shaikh M. Formulation, optimization, and characterization of biocompatible inhalable D-Cycloserine-loaded alginate-chitosan nanoparticles for pulmonary drug delivery. *Asian J Pharm Clin Res* 2016;9:82-95.
  27. Sailaja AK, Amareshwar P. Preparation of alginate nanoparticles by desolvation technique using acetone as desolvating agent. *Asian J Pharm Clin Res* 2012;5:132-4.